Supporting information for

Photothermally driven decoupling of gas evolution from solid-liquid interface for boosted photocatalytic hydrogen production

Shidong Zhao[a,†], Chunyang Zhang[a,†], Shujian Wang[a,†], Kejian Lu[a,], Biao Wang[a,], Jie Huang[a,], Hao Peng[a,], Naixu Li[c,], Maochang Liu[a,b]*

[a]*International Research Center for Renewable Energy, State Key Laboratory of Multiphase Flow in Power Engineering, Xi'an Jiaotong University, Xi'an, Shaanxi 710049, P. R. China*

[b]*Suzhou Academy of Xi'an Jiaotong University, Suzhou, Jiangsu 215123, P. R. China*

[c]*School of Chemistry and Chemical Engineering, Southeast University, No.2 Dongnandaxue Road, Nanjing 211189, Jiangsu, P. R. China*

†These authors contribute equally.

*To whom correspondence should be addressed. E-mail: maochangliu@mail.xjtu.edu.cn.

Methods

Chemicals and materials

All chemicals, including Cadmium nitrate tetrahydrate ($Cd(NO_3)_2 \cdot 4H_2O$), thiourea (NH_2CSNH_2), Nickel acetate tetrahydrate ($Ni(CH_3COO)_2 \cdot 4H_2O$), ethylenediamine ($H_2NCH_2CH_2NH_2$), triethanolamine ($C_6H_{15}NO_3$), dimethylformamide (DMF) and polyvinylidene fluoride (PVDF) were purchased from Sinopharm Chemical Reagent Co., LTD and were analytical grade without further purification. Melamine sponge was purchased from Shanghai Beyou Building Materials Co., LTD. The water used in experiments is deionized water with a resistivity of 18.25 MΩ cm.

Synthesis of CdS nanorods

In a typical procedure, 10 mmol $Cd(NO_3)_2 \cdot 4H_2O$ and 30 mmol NH_2CSNH_2 were dissolved in 60 mL ethylenediamine under intense stirring. After stirring for 30 min, the reaction mixture was transferred into a 100-ml-capacity Teflon-lined autoclave and heated at 160 °C for 48 h. When the autoclave cooled down to room temperature naturally, the yellow precipitate was collected by centrifugation and washed with deionized water and ethanol several times. The collected solid was dried in a vacuum oven at 60 °C for 8 h to obtain CdS nanorods.

Synthesis of various Ni-containing CdS photocatalysts

The Ni-containing CdS photocatalyst was obtained using a photodeposition method in a 220 ml sealed Pyrex reactor. Typically, CdS photocatalyst with different contents of Ni (0.1 wt.%, 0.5 wt.%, 1 wt.%, 2 wt.% and 3wt.%) were synthesized using the following procedure: different contents of $Ni(CH_3COO)_2 \cdot 4H_2O$ and 200 mg CdS powder were added to a mixed solvent containing 162 mL deionized water and 18 mL triethanolamine by stirring for 30 min. To remove any residual air the reactor was purged with argon for 30 min before the photodeposition reaction. Subsequently, the reaction mixture was irradiated under UV-visible light for 1 h to sufficiently reduce the Ni ions. The temperature of the reaction solution was kept at 35 °C by a circulating water pump throughout the whole experiment. Finally, the product was separated by centrifugation, washed several times with deionized water and ethanol, and dried at 60 °C for 6 h in a vacuum oven. The resulting sample was named xNC,

where x represents the weight ratio of Ni to CdS.

Preparation of annealed melamine sponges in air

Pristine melamine sponge (MS) with size of 6 cm × 6 cm × 4 cm were put into a muffle furnace and annealed at 400 °C for 1 h with a ramping rate of 10 °C min^{-1}. After cooling, the annealed melamine sponge (AMS) was obtained.

Synthesis of photocatalysts/AMS systems

First, the bulk AMS was cut into a cylinder with a diameter of 3 cm and a thickness of 2.5 cm. Subsequently, photocatalyst such as CdS nanorods (50 mg) was dispersed in 5 mL dimethylformamide (DMF) solution containing PVDF (30 mg ml^{-1}) by ultrasonication and stirring for 20 min. Subsequently, the obtained mixed solution was evenly coated on the surface of AMS with a pipette gun. Eventually, the resulting CdS/AMS system was dried in a vacuum oven at 80 °C for 10 h. The preparation method of 1NC/AMS, CdS/MS and1NC/MS system is the same with that of CdS/AMS system.

Characterizations

The scanning electron microscopy (SEM) images of the catalysts were recorded on a SEM (JEOL 7800F) equipped with an EDX spectrometer. The morphology of the sample was characterized on transmission electron microscopy (TEM) (G2F30) combined with the OXFORD MAX-80 energy-dispersive X-ray detector (EDX). Raman spectra was obtained on a spectrometer (LabRAM HR 800, Horiba/Jobin Yvon, France) using a laser excitation of 638 nm. Optical properties were determined by a Hitachi double-beam U-4100 UV–vis-near-IR spectrophotometer equipped with an integrating sphere in which $BaSO_4$ acted as the background. X-ray diffraction patterns were collected using a PANalytical X'Pert Pro MPD diffractometer operated at 40 kV and 40 mA using Ni-filtered Cu Kα irradiation (λ = 1.5406 Å). X-ray photoelectron spectroscopy (XPS) patterns of the samples were recorded from AXIS Ultra DLD Kratos spectrometer with a standard and monochromatic Al Kα radiation. The C1s peak at 284.8 eV of adventitious carbon was used for calibration. The steady-state PL emission spectra and time-resolved transient PL decay spectra were measured at room temperature using a PTI QM-4 fluorescence spectrophotometer.

Photoelectrochemical measurements

The photoelectrochemical performance was measured using CHI760D electrochemical

workstation in the standard three-electrode system with a working electrode of the samples, a reference electrode of Ag/AgCl in saturated KCl and a counter electrode of Pt. A 300W Xe lamp was used as the light source and a 0.5 M Na_2SO_4 was used as the electrolyte. For preparing the working electrodes, 1 mg of as-synthesized sample and 10 μL of 10% Nafion (DuPont) were uniformly dispersed in 1.0 mL of water/ethanol (volume ratio: 1/1) mixture solution. Subsequently, the mixture was treated under ultrasonication for 1 h to get the homogeneous suspension and 100 μL of resultant suspension was uniformly dropped onto the surface of a 3 × 1 cm^2 FTO glass plate with working area of 2 cm^2. Finally, the FTO glass plate was heated to form a sample film to obtain a working electrode.

Solar–driven water evaporation measurements

The solar-driven water evaporation experiments were conducted at room temperature under the simulated sunlight illumination (AM 1.5G) of one-sun intensity. The incident power density of solar illumination was accurately measured by photometer. A 1NC/MS or 1NC/AMS system with a surface area of 7.07 cm^2 was used as an evaporation device. The water weight loss was recorded by an electrical balance every 10 min. The solar photothermal conversion efficiency η was evaluated according to the following equation: [1]

$$\eta = \frac{mh_{lv}}{q_i} \#(1)$$

where m is the solar-driven evaporation rate of water under solar illumination, q_i is the incident power density of solar illumination in process of vapor generation experiment, and h_{lv} made up of the sensible heat and the enthalpy of vaporization is calculated using the Equation (2):

$$h_{lv} = C\Delta T + \Delta h \#(2)$$

Where C is the specific heat capacity of water and a constant of 4.18 J g^{-1} K^{-1}, ΔT is the temperature increase of water, and Δh is the enthalpy of vaporization on the relative temperature.

Photocatalytic measurements

The decoupling reaction system of photothermally induced liquid-solid/gas-solid was shown in Fig. 4a. The prepared photocatalysts/AMS system was semi immersed in 30ml

triethanolamine aqueous solution (10%, 27 mL of H_2O and 3 mL of triethanolamine). Then the mixed system was purged with argon for 30 min to remove air. A 300W Xe lamp was used as the light source (λ > 300 nm) to trigger the photocatalytic generation of H_2. The overall ambient temperature of the reaction was kept at 35 °C by a circulating water pump throughout the whole experiment. For the triphase CdS nanorods system, photocatalyst powder (50 mg) was dispersed by a magnetic stirrer in solution 30 ml triethanolamine aqueous solution (10%, 27 mL of H_2O and 3 mL of triethanolamine), and other reaction conditions were consistent with the photocatalysts/AMS system. The STH efficiency was determined according to the following equation:

$$STH(\%) = \frac{Evolved\ hydrogen\ amount \times \Delta G_r}{P \times S \times t} \#(3)$$

Here, ΔG_r, P, S and t denote the reaction Gibbs energy for the water splitting reaction, the power of solar irradiation, the irradiated area and the time of reaction, respectively. The value of ΔG_r used for the calculations were 237 kJ mol^{-1} for the liquid water in the triphase reaction system, and 229 kJ mol^{-1} for the water vapor in the liquid-solid/gas-solid decoupling reaction system. [2, 3]

Calculation details

The Vienna Abinitio Simulation Package (VASP) based on Density functional theory (DFT) was employed in the entire calculations. [4-7] Perdew-Burke-Ernzerhof exchange-correlation functional within generalized gradient approximation was applied while a plane-wave basis set was implemented in the framework of the projector augmented wave (PAW) method to represented the core and valence electrons with a kinetic cutoff energy of 400 eV. [8, 9] The atomic structures were fully relaxed until energy and forces were converged to 10^{-5} eV $Å^{-1}$ and 0.02 eV $Å^{-1}$, respectively. The surface model of 1NC draws on the work of Wang et. al. [10] A 3×5×1 Monkhorst-Pack k-point mesh was employed to sample the Brillouin zone for all surface model. All calculations were performed on a (100) slab model with 2 × 1 surface cell. Six atomic layers were used for the surface models and the four bottom layers were fixed throughout the calculations. To avoid the periodic interaction along out-plane direction, a vacuum layer of 15 Å was used for the slab model.

Generally, HER process includes the following processes under acidic conditions:

$$* + H_2O + e^- = *H + OH^- \qquad (Volmer)\#(4)$$

$$*H + H_2O + e^- = * + OH^- + H_2 \qquad (Heyrovsky)\#(5)$$

or

$$2*H = 2* + H_2 \qquad (Tafel)\#(6)$$

The atom H, OH or H_2O adsorption free energy (ΔG_s) on disparate active sites can be defined as equation (4):

$$\Delta G_s = \Delta E_s + \Delta E_{ZPE} - T\Delta S_s \qquad \#(7)$$

Where ΔE_s is the hydrogen absorption energy, ΔE_{ZPE} is the difference in zero point energy between the surface species and dissociative species, T is the temperature (degree kelvin, K), and S_s is the entropy change between the adsorbed state of the system and the gas phase standard state. By consulting the Handbook of Chemistry and Physics, we can get the entropy change of water in the liquid and gas phases. [11] The entropy S is 69.950 J mol^{-1} K^{-1} at 298.15 K under the standard pressure. At 373.15 K, the entropy S is 86.896 J mol^{-1} K^{-1} when the water is liquid, while the entropy S is 196.631 J mol^{-1} K^{-1} when the water is in the gas phase. At this point, the ΔG_s of different sites can be acquired. Vaspkit code is used for post-computation. [12]

Table S1. Kinetic parameters of the charge carrier decay in CdS and 1NC.

Samples	τ_1 (ns)	A_1	τ_2 (ns)	A_2	τ_3 (ns)	A_3	τ_{avg} (ns)	χ^2
CdS	0.2688	0.4108	2.7800	0.3549	16.4092	0.2343	4.94	1.1596
1NC	0.2375	0.6086	3.3117	0.2547	34.4070	0.1366	5.69	1.2819

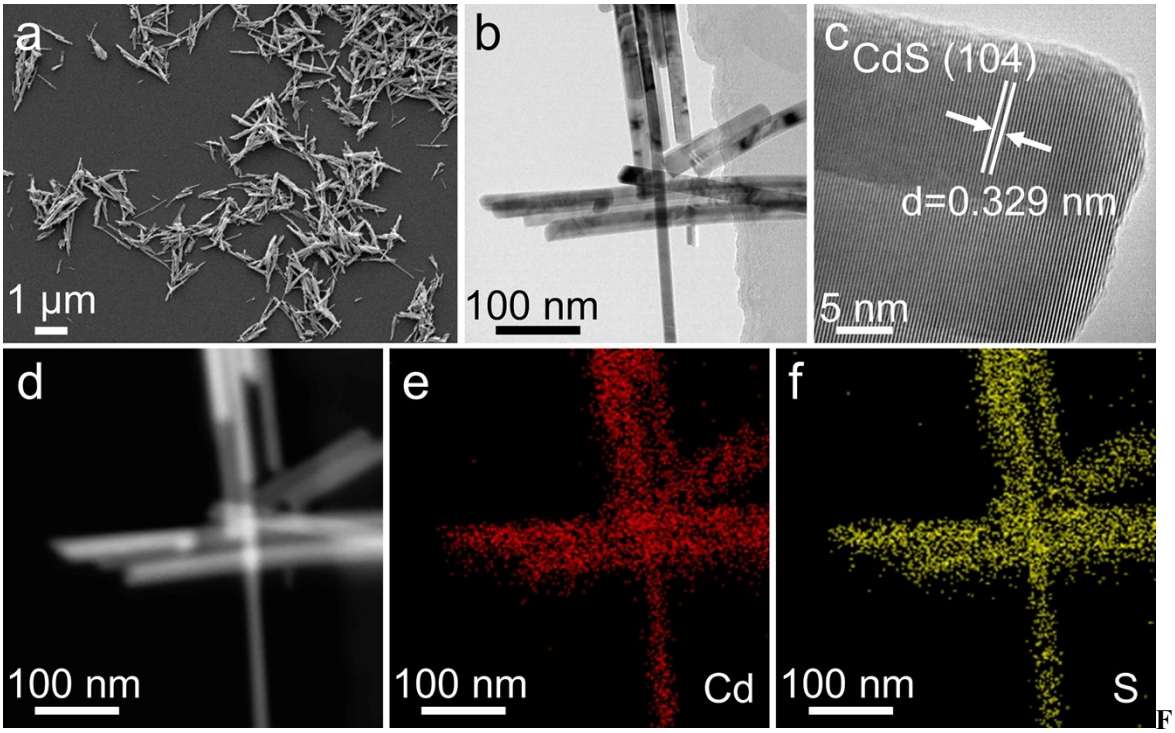

Figure S1. a) SEM image, b) TEM image and c) HRTEM image of CdS. d-f) Elemental mapping images of CdS. d) Selected area, e) Cd element, f) S element.

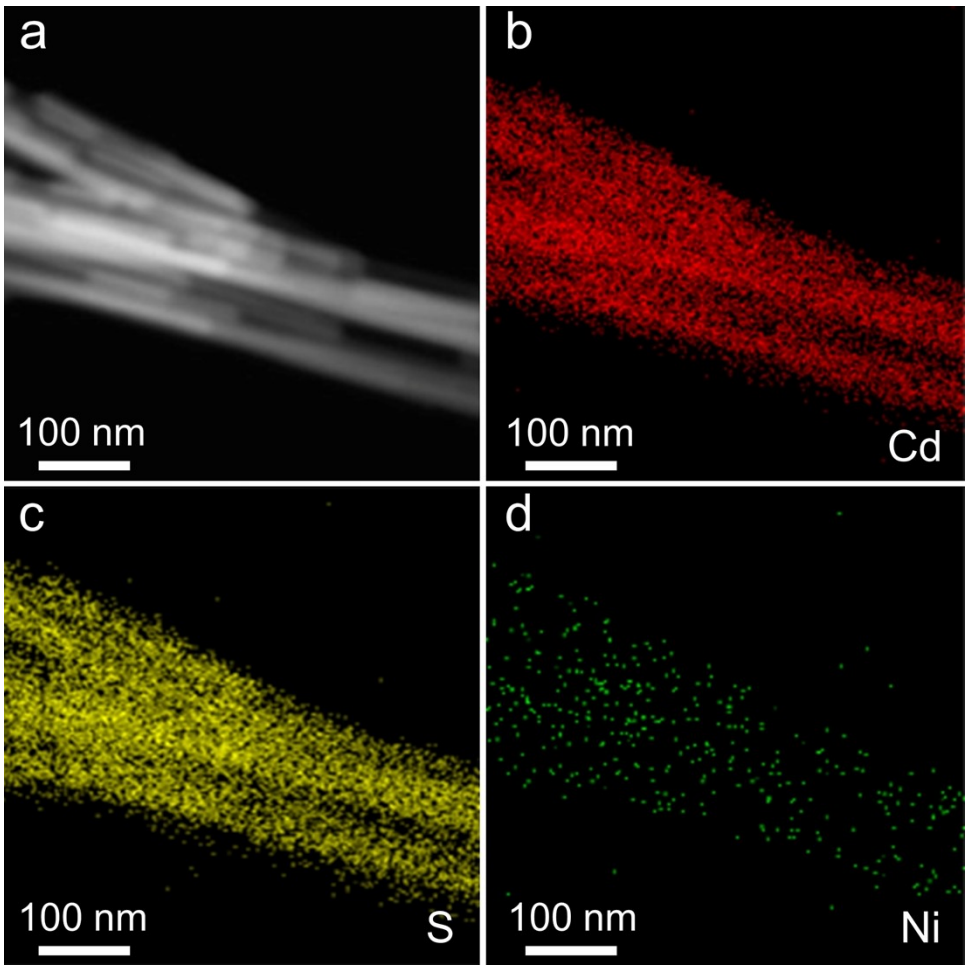

Figure S2. a-d) Elemental mapping images of 1NC. a) Selected area, b) Cd element, c) S element, d) Ni element.

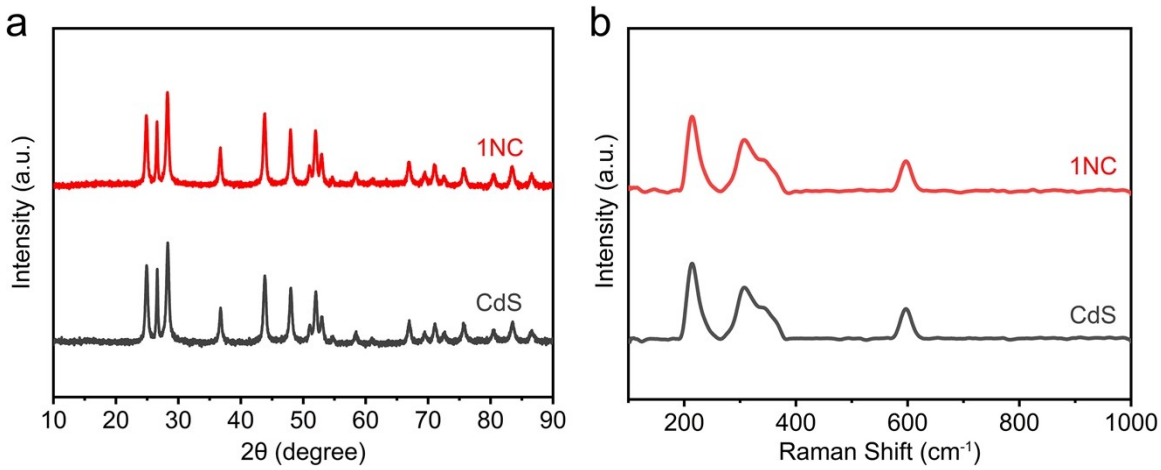

Figure S3. a) XRD patterns and b) Raman spectra of CdS and 1NC.

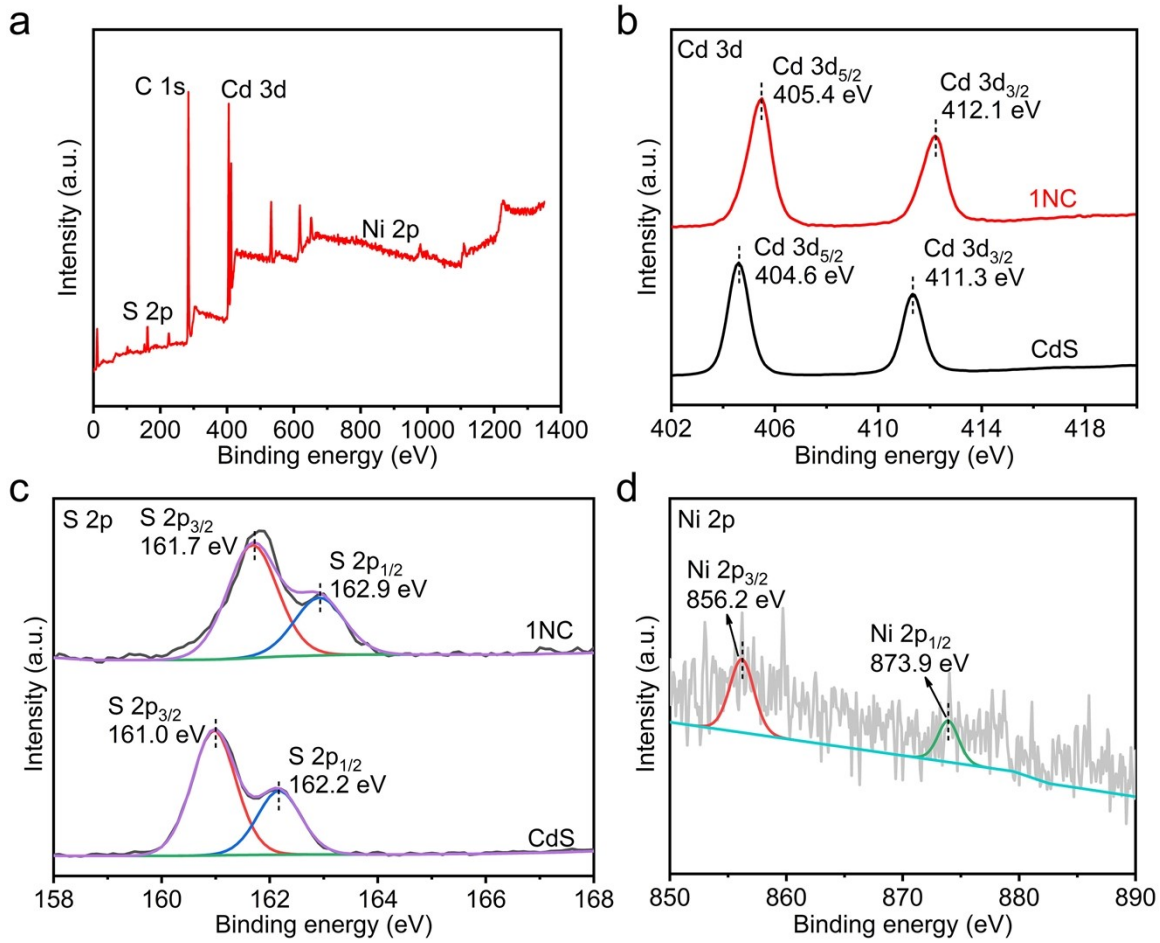

Figure S4. a) XPS survey spectra of 1NC. b) Cd 3d and c) S 2p high-resolution XPS spectra of CdS and 1NC. d) Ni 2p high-resolution XPS spectrum of 1NC.

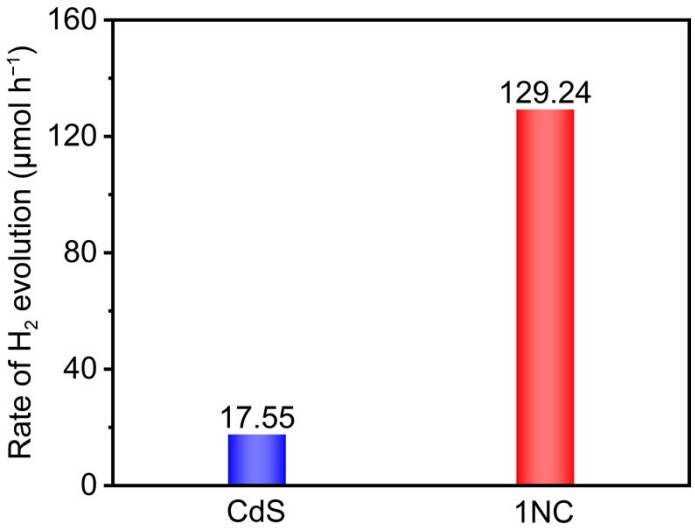

Figure S5. Comparison of hydrogen evolution rates between CdS and 1NC in the triphase system.

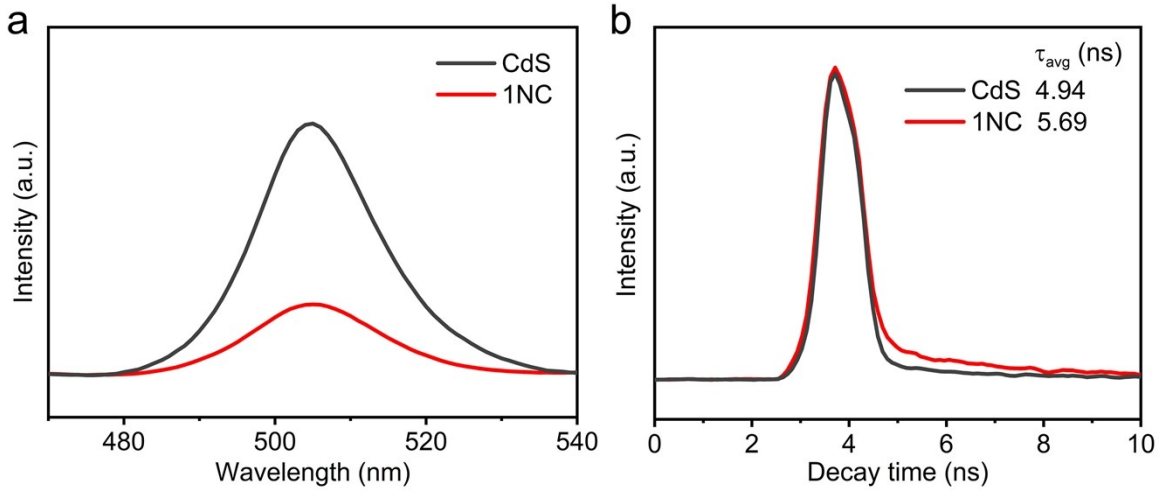

Figure S6. a) Steady-state photoluminescence emission spectra and b) time-resolved transient PL decay spectra of CdS and 1NC at room temperature. The excitation wavelength for all samples is 400 nm.

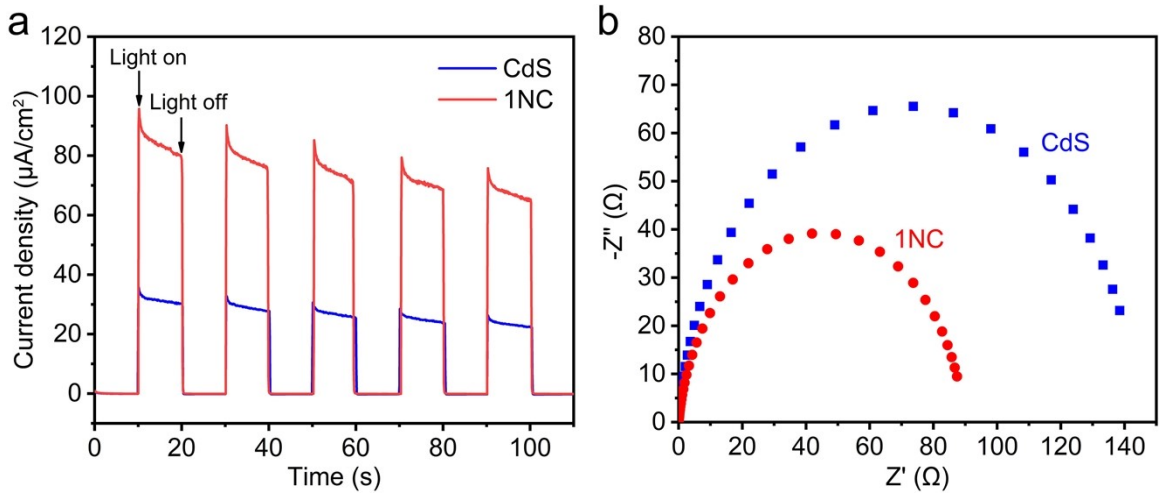

Figure S7. a) Photocurrent response versus time and b) EIS curves of as-prepared CdS and 1NC.

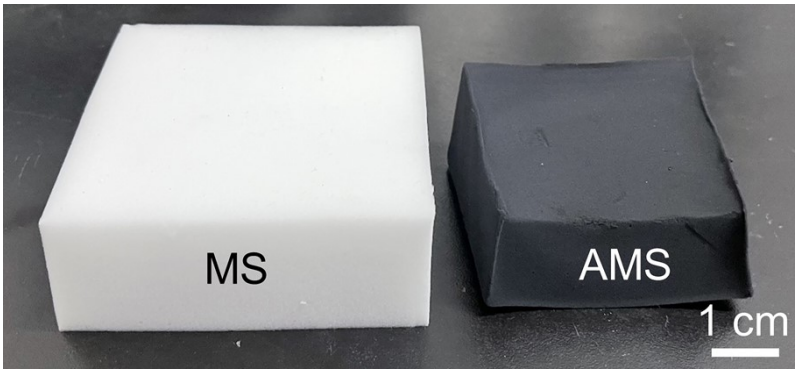

Figure S8. Photo of melamine sponge before and after annealing.

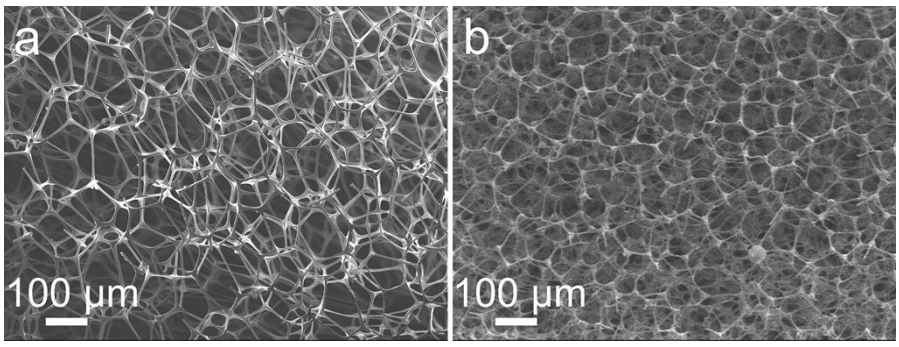

Figure S9. SEM images of a) MS, and b) AMS at the same magnification.

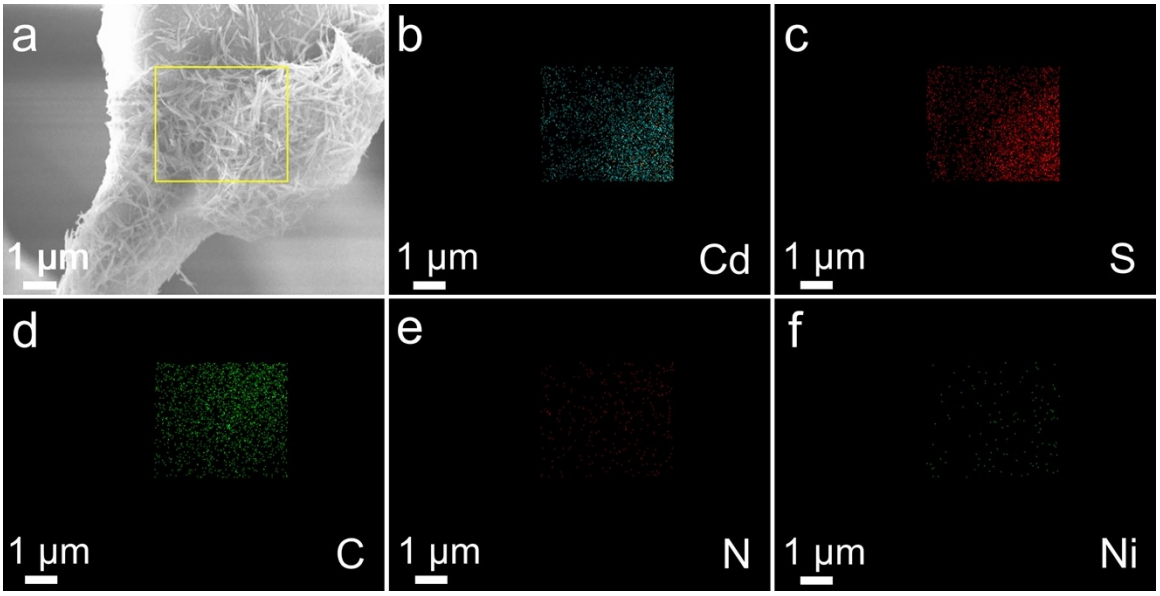

Figure S10. a) SEM image of the 1NC/AMS, and the corresponding elemental mapping images of b) Cd, c) S, d) C, e) N, and f) Ni.

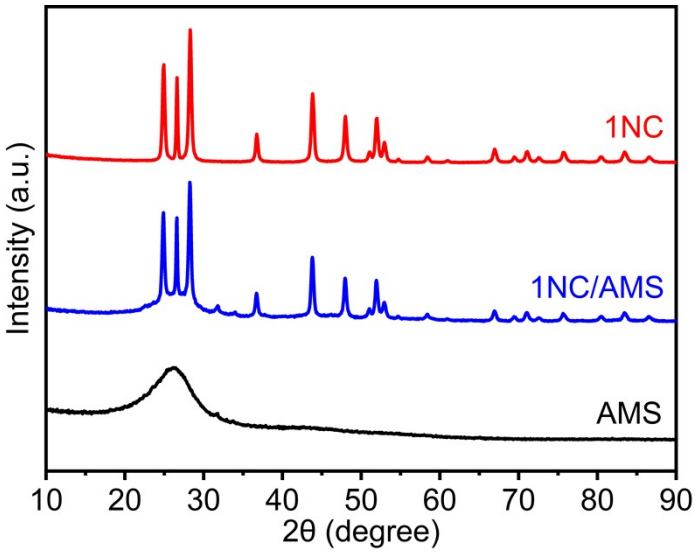

Figure S11. XRD patterns of 1NC, AMS and 1NC/AMS.

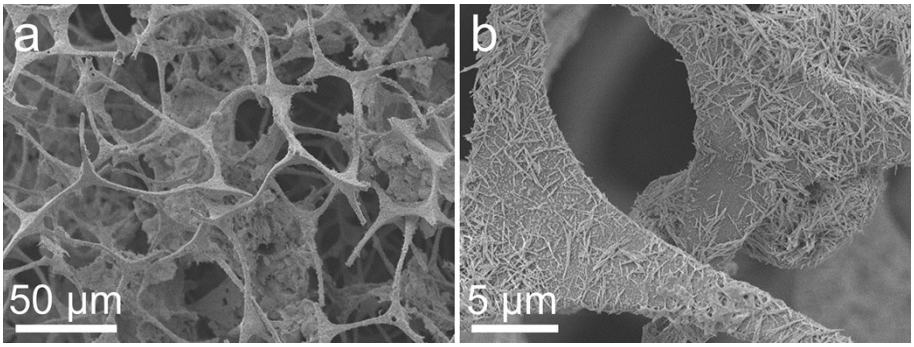

Figure S12. a,b) SEM images of the CdS/AMS at different magnification.

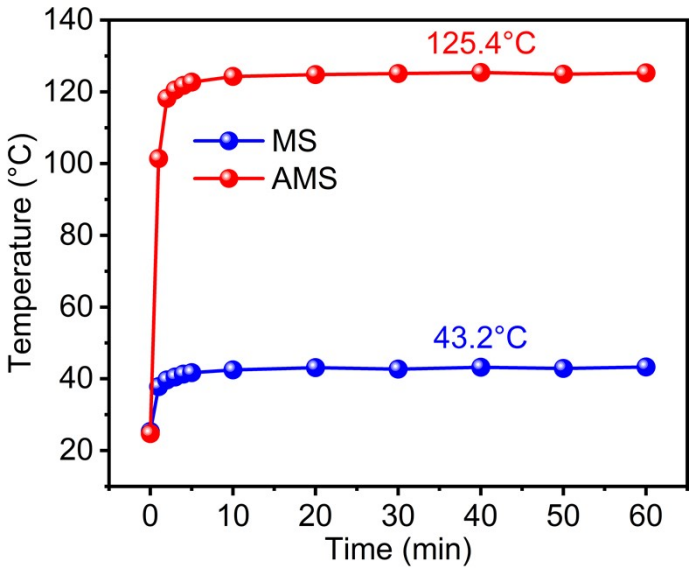

Figure S13. Surface temperature changes of MS and AMS in air under one-sun illumination.

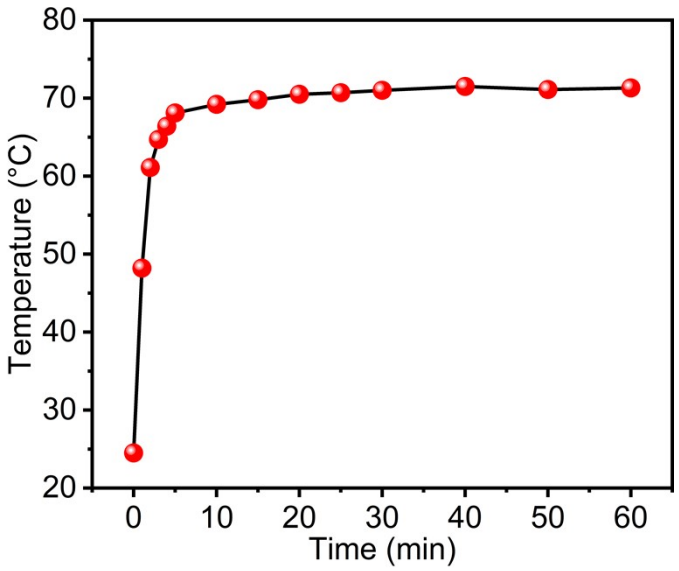

Figure S14. Surface temperature change of 1NC/AMS during photocatalytic hydrogen evolution.

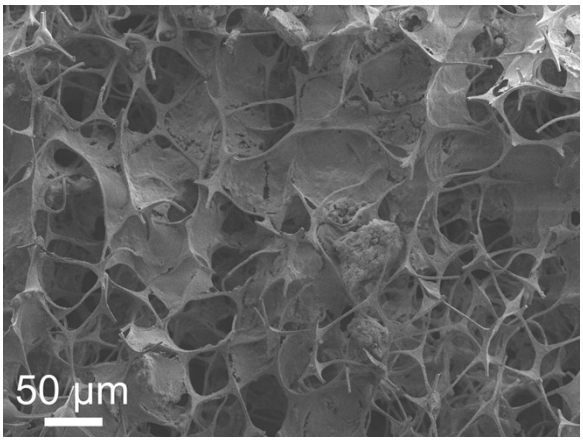

Figure S15. SEM image of CdS/AMS composite with 80 mg of photocatalyst loaded.

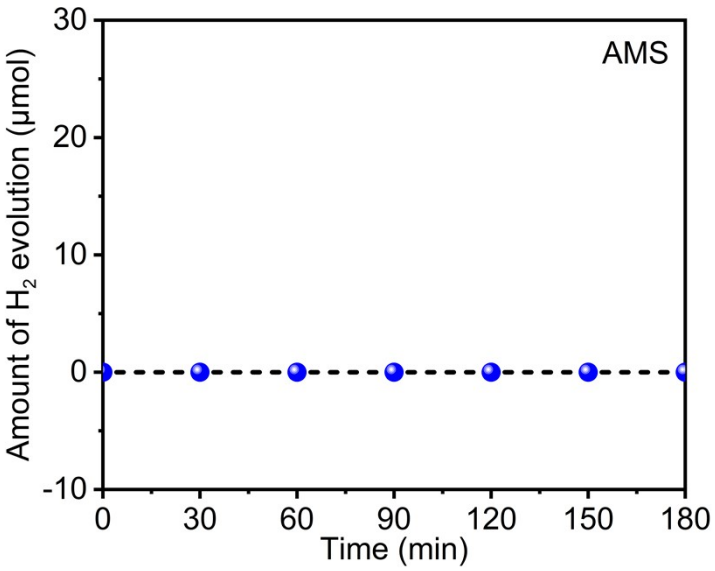

Figure S16. Time courses for photocatalytic hydrogen evolution based on AMS.

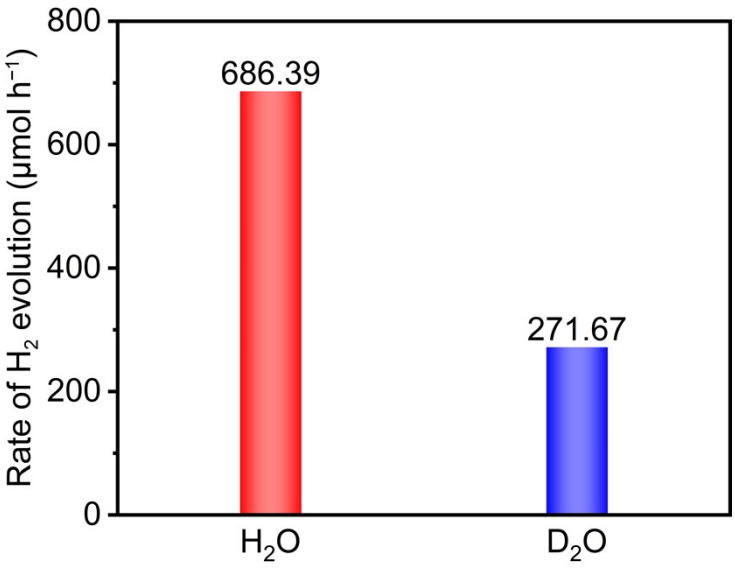

Figure S17. Comparison of hydrogen evolution rates of 1NC/AMS system under different water sources.

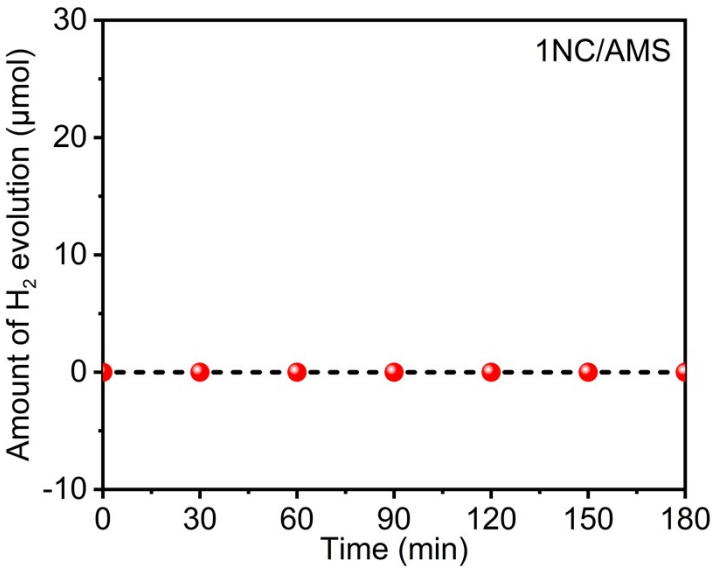

Figure S18. Time-dependent photocatalytic hydrogen evolution curve of 1NC/AMS at 70 ℃ without light illumination.

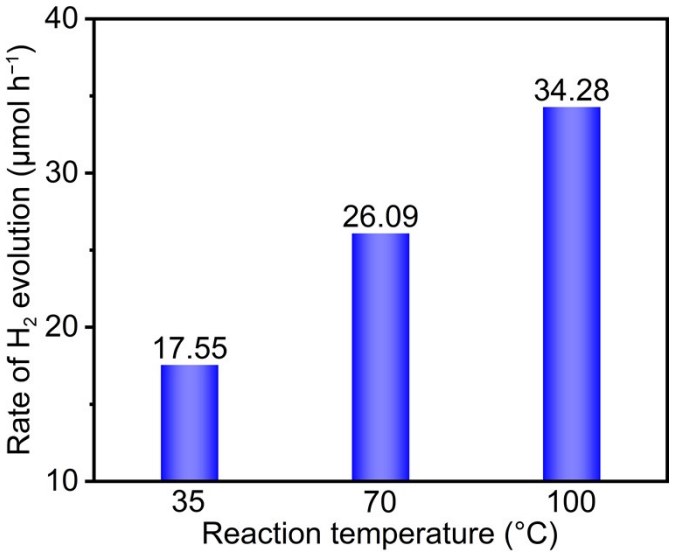

Figure S19. Temperature-dependent photocatalytic hydrogen evolution rates for the triphase CdS nanorods system.

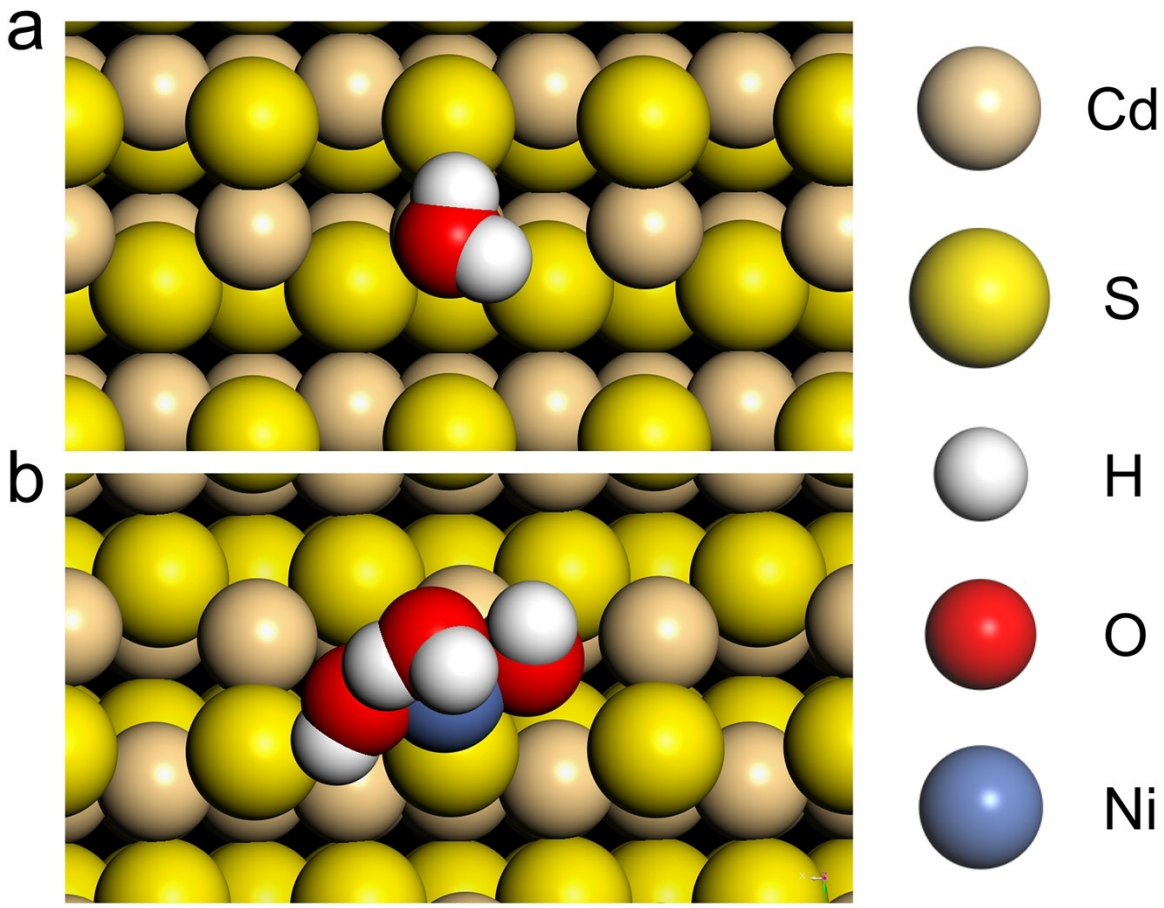

Figure S20. Optimal water molecular adsorption configuration on a) CdS and b) 1NC.

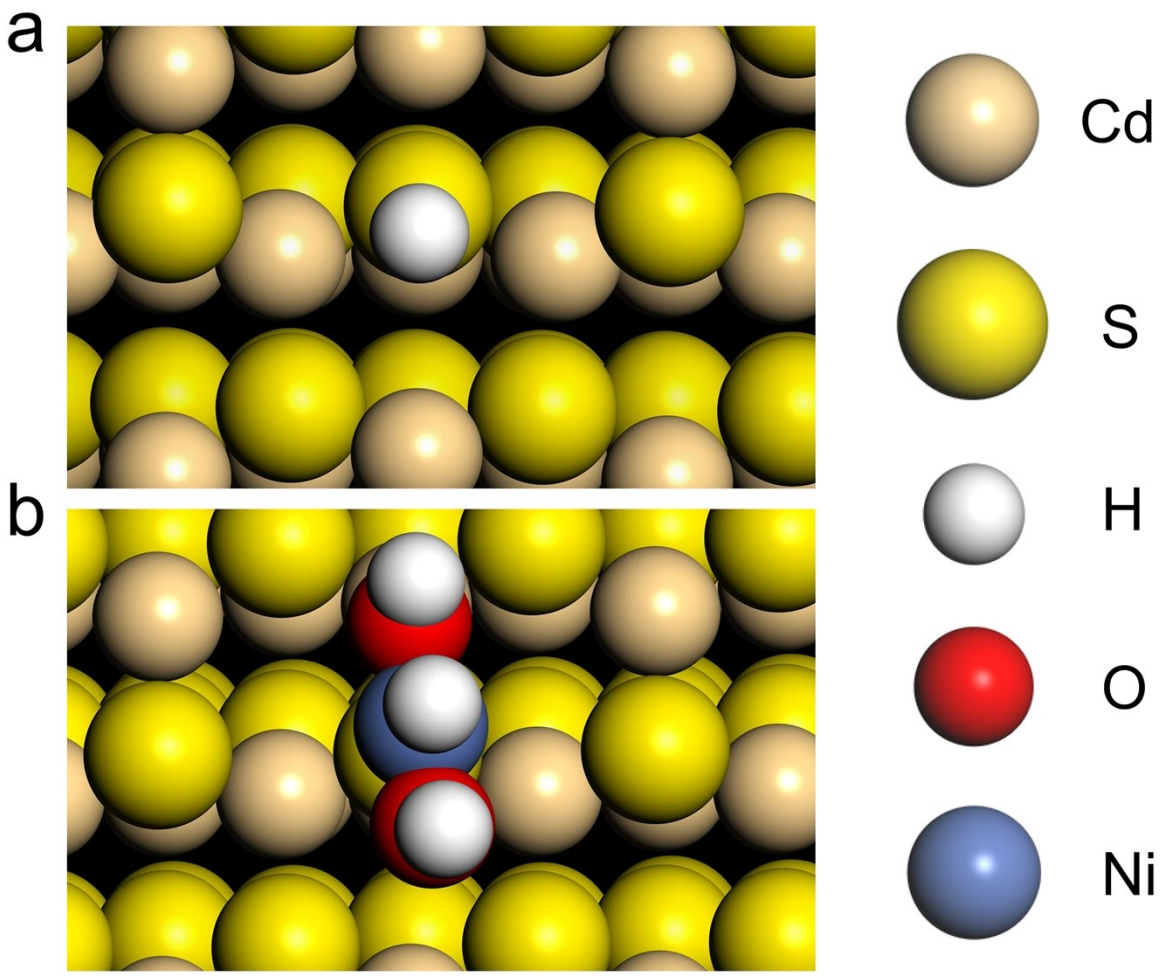

Figure S21. Optimal hydrogen adsorption configuration on a) CdS and b) 1NC.

References

1. X. Li, W. Xu, M. Tang, L. Zhou, B. Zhu, S. Zhu and J. Zhu, *Proc Natl Acad Sci U S A*, 2016, **113**, 13953-13958.

2. M. A. Modestino, M. Dumortier, S. M. Hosseini Hashemi, S. Haussener, C. Moser and D. Psaltis, *Lab Chip*, 2015, **15**, 2287-2296.

3. J. M. Spurgeon and N. S. Lewis, *Energy & Environmental Science*, 2011, **4**, 2993-2998.

4. G. Kresse and J. Furthmuller, *Phys. Rev. B*, 1996, **54**, 11169-11186

5. G. Kresse and J. Furthmuller, *Comput. Mater. Sci.*, 1996, **6**, 15-50.

6. M. Hacene, A. Anciaux-Sedrakian, X. Rozanska, D. Klahr, T. Guignon and P. Fleurat-Lessard, *J Comput Chem*, 2012, **33**, 2581-2589.

7. M. Hutchinson and M. Widom, *Computer Physics Communications*, 2012, **183**, 1422-1426.

8. J. P. Perdew, K. Burke and M. Ernzerhof, *Phys. Rev. Lett.*, 1996, **77**, 3865-3868.

9. H. J. Monkhorst and J. D. Pack, *Phys. Rev. B*, 1976, **13**, 5188-5192.

10. H. Z. Zhang, Y. M. Dong, S. Zhao, G. L. Wang, P. P. Jiang, J. Zhong and Y. F. Zhu, *Appl. Catal., B*, 2020, **261**, 118233.

11. D. R. Lide, *Handbook of Chemistry and Physics*, CRC Press, Boca Raton, 2004.

12. V. Wang, N. Xu, J. C. Liu, G. Tang and W. T. Geng, *Computer Physics Communications*, 2021, **267**, 108033.